A SPATIALLY ADAPTIVE HIERARCHICAL STOCHASTIC MODEL FOR NON-RIGID IMAGE REGISTRATION

Evangelos Fotiou , Christophoros Nikou and Nikolaos Galatsanos

University of Ioannina,
Department of Computer Science,
PO Box 1185, 45110 Ioannina, Greece,
{efotiou, cnikou, galatsanos}@cs.uoi.gr

ABSTRACT

In this paper, we propose a method for non-rigid image registration based on a spatially adaptive stochastic model. A smoothness constraint is imposed on the deformation field between the two images which is assumed to be a random variable following a Gaussian distribution, conditioned on the observations and maximum *a posteriori* (MAP) estimation is employed to evaluate the model parameters. Furthermore, the model is enriched by considering the deformation field to be spatially adaptive by assuming different density parameters for each image location. These parameters are assumed random variables generated by a Gamma distribution, which is conjugate to the Gaussian, leading to a model that can be estimated. Numerical experiments are presented that demonstrate the advantages of this model.

1. INTRODUCTION

Image registration is the process of determining an appropriate transformation function which, applied to the coordinates of one image (source image), aligns it with another (target image). It is used either in an intra or an inter-subject level. The involved transformations are divided into two main categories: rigid and non-rigid. Rigid transformations preserve the distance between all points in an image and can be represented by shifting and rotating a cartesian system. In the non-rigid case, straight lines are mapped to curves, increasing the degrees of freedom of the problem and, consequently, making it more difficult to solve. Medical imaging is one of the main, if not the most important, application fields of non-rigid image registration [8].

Non-rigid image registration methods [15] may be grouped in two main subcategories, according to their theoretical foundation. In the first subcategory the deformation is modeled using a set of basis functions. These can be B-splines [18], wavelets [21] or radial basis functions [11]. On the other hand, there are methods that connect the image data with a physically deforming system. They use concepts from continuum mechanics to model the source image as a version of the target, embedded into a deformable medium. The medium is then deformed subject to internal forces which result in the reconfiguration to its original state (target image). Well known methods are based on physical models such as linear elasticity [9], viscus fluid flow [5] and optical flow [19].

Non-rigid image registration yields a nonlinear ill-posed inverse problem that require regularization [20]. Minimization of the energy functional in the intensity based methods, locates the optimal transformation function out of the space of all admissible solutions. Even when local minima are avoided, the transformation does not necessarily preserve the topology of the image data. Topology preserving mapping is required especially in inter-subject registration of medical images, since anatomical structures have the same topology for any individual. As a result, further constraints have to be introduced, in order to restrict the space of admissible solutions to those which provide anatomically coherent transformations. In the physical models such as linear elasticity, these constraints arise naturally, while another popular choice is the Laplacian constraint [2]. Once the constraint is chosen, it is minimized simultaneously with the energy functional [7]. However, for large non-rigid transformations, this leads to large computational cost, since the constraint, in the linear regularization models, generally increases proportionally to the deformation magnitude. Multiresolution techniques, where coarse to fine strategies are used, have been reported to reduce the computational demands [16]. Even in that case, the task of estimating a transformation which provides both satisfactory and topology preserving mapping is nontrivial. Inducing further restrictions to the above models, such as setting the transformation to be diffeomorphic, seems to result in topology preserving transformations [14]. However, in this case, the need to track the discrete Jacobian of the transformation can be an important drawback. Similar in spirit approaches were also proposed in [12, 1, 17].

In the present study, we propose a method motivated by the constrained optical flow formulation for image registration [13]. At first, we impose a smoothness constraint on the deformation field. Also, the deformation field is assumed to be a random variable following a Gaussian pdf and we recur to the maximum *a posteriori* (MAP) formulation in order to evaluate the model parameters. Moreover, we assume a more flexible model by considering different pdf parameters for each image location, thus, making the model *spatially adaptive*. In the remainder of this paper, we present our spatially adative model in section 2, numerical results and discussion on the advantages and of the proposed model with respect to both the constrained optical flow and the simple non adaptive model are presented in section 3.

2. REGISTRATION METHOD

2.1 Problem formulation

Let $A(\mathbf{s}) = A(x,y)$ be the target image and $B(\mathbf{s}) = B(x,y)$ the source image to be aligned with A. We assume that we are dealing with a single-modal image registration problem. Our objective is to estimate a displacement field $\mathbf{u}$, which

minimizes the energy function E between the two images:

$$E(\mathbf{u}) = \int_{\mathbf{\Omega}} \|B(\mathbf{s}+\mathbf{u}(\mathbf{s})) - A(\mathbf{s})\|^2 \mathbf{ds} \quad (1)$$

where $\mathbf{\Omega}$ is the bounded domain defined by the images and $\mathbf{s} = (x, y)$ is the position vector for a given pixel. Under the assumption that the target image is a geometrically deformed version of the source image with i.i.d. (independent and identically distributed) Gaussian noise added to each pixel, minimization of (1) yields to the optimal solution in the *maximum likelihood* sense.

Vectorizing the two images, we get two N-dimensional discrete signals a(i) and $b(i)$ where $i \in I \subset \mathbb{Z}^N$, and I is an N-dimensional discrete interval representing the set of all pixel coordinates in the image. The deformation field is also vectorized in the form $\mathbf{u} = (\mathbf{u_x u_y})^\mathbf{T}$, where $\mathbf{u_x}$,$\mathbf{u_y} \in \mathbb{R}^\mathbf{N}$. For simplicity from now on $\mathbf{u}(\mathbf{s}) = \mathbf{u}$.

First, we summarize the optical flow model for image registration. In this model we start by retaining the first-order terms of the Taylor expansion of the intensity function in the source image.

$$b(\mathbf{s}+\mathbf{u}) = b(\mathbf{s}) + \mathbf{u}^T \nabla b(\mathbf{s}) + \varepsilon(\mathbf{s}), \quad (2)$$

where $\varepsilon(\mathbf{s})$ the residual of the Taylor expansion and is assumed small. We assume

$$b(\mathbf{s}+\mathbf{u}) - \mathrm{a}(\mathbf{s}) \simeq 0, \quad (3)$$

or

$$b(\mathbf{s}) + \mathbf{u}^T \nabla b(\mathbf{s}) - \mathrm{a}(\mathbf{s}) = -\varepsilon(\mathbf{s}), \quad (4)$$

or

$$d(\mathbf{s}) + \mathbf{u}^T \nabla b(\mathbf{s}) = -\varepsilon(\mathbf{s}), \quad (5)$$

where $d(\mathbf{s}) = b(\mathbf{s}) - \mathrm{a}(\mathbf{s})$, is the intensity difference between source and target image. Using this approximation we obtain a displacement field to be applied in the source image. This field implies a displacement in the direction of $\nabla b(\mathbf{s})$ and its orientation is $+\nabla b(\mathbf{s})$ if $b(\mathbf{s}) < \mathrm{a}(\mathbf{s})$ and $-\nabla b(\mathbf{s})$ otherwise. No displacement occurs wherever the two intensities match.

The main disadvantage of this model is that since there are no constraints in the deformation field, equation (5) does not have a unique solution. In other words, from N observations stacked in vector $\mathbf{d}$, $2N$ parameters stacked in vectors $\mathbf{u_x}$, $\mathbf{u_y}$ have to be estimated. This is an ill-posed problem that requires regularization [20]. In this study, we apply the Laplacian operator on the displacement field and then use the Euclidian norm of the product for regularization. In subsection 2.2 we present a generalization of the above model which uses concepts from stochastic estimation theory.

Let $\mathbf{g}(\mathbf{s}) = \nabla B(\mathbf{s})$ and $\mathbf{Q} = \nabla^\mathbf{2}$ be the Laplacian operator. Applying the optical flow model using, in the sense mentioned above, the Laplacian operator as a constraint for Tikhonov regularization, we come up with the following minimization problem.

$$\mathbf{u} = \arg\min_{\mathbf{u}} [\| \mathbf{d} + \mathbf{G}\mathbf{u} \|^2 + \alpha \| \mathbf{Q}\mathbf{u} \|^2] \quad (6)$$

where α is a weight factor,

$$\mathbf{d} = (d_1 d_2 ... d_N)^T \quad (7)$$

is a vector containing the temporal image differences and

$$\mathbf{G} = diag\{g_{x1}, g_{x2}, ..., g_{xN}, g_{y1}, g_{y2}, ..., g_{yN}\} \quad (8)$$

is a matrix containing the image gradient with respect to the horizontal and vertical directions. Taking the above formulation into account and minimizing equation (6) with respect to $\mathbf{u}$ yields:

$$(\mathbf{G}\mathbf{G}^T + \alpha \mathbf{Q}^T \mathbf{Q})\mathbf{u} = -\mathbf{G}\mathbf{d}. \quad (9)$$

Due to the high dimensionality of the involved matrices, the above linear system may be approximately solved using the Conjugate Gradients Squared method (CGS). Once we obtain the deformation field $\mathbf{u}$, we compute the deformed source image b^* through cubic interpolation. The algorithm iterates over time, producing an increasing deformation field after each iteration. At the end of each iteration the deformed image b^* is resampled and used as the source image for the next iteration.

2.2 Spatially adaptive model

It is well known that Tikhonov regularization has also a stochastic interpretation using MAP estimation and introducing an appropriate prior [10]. In this framework, we assign a Gaussian prior probability distribution $p(\mathbf{u})$ to the elements of the deformation field. In our case, the observed data set is the vector with elements the differences in intensity for each pixel $\mathbf{d} = (d_1 d_2 ... d_N)^T$. The *likelihood function* $p(\mathbf{d}|\mathbf{u})$ is related to the *posterior probability* $p(\mathbf{u}|\mathbf{d})$ through Bayes' theorem:

$$p(\mathbf{u}|\mathbf{d}) \propto p(\mathbf{d}|\mathbf{u}) p(\mathbf{u}) \quad (10)$$

We can now determine $\mathbf{u}$ by finding the most probable value of $\mathbf{u}$ given the observations by MAP estimation.

The Gaussian pdf for a N-dimensional vector $\mathbf{x}$ of continuous variables is expressed by

$$\mathcal{N}(\mathbf{x}; \mu, \mathbf{\Sigma}) = \frac{\mathbf{1}}{(\mathbf{2}\pi)^{\frac{\mathbf{N}}{\mathbf{2}}} |\mathbf{\Sigma}|^{\frac{\mathbf{1}}{\mathbf{2}}}} \mathbf{exp}^{-\frac{\mathbf{1}}{\mathbf{2}}(\mathbf{x}-\mu)^\mathbf{T} \mathbf{\Sigma}^{-\mathbf{1}} (\mathbf{x}-\mu)} \quad (11)$$

where N is the dimensionality of the vector and μ, $\mathbf{\Sigma}$ are the mean vector and covariance matrix respectively. The inverse of the covariance matrix is known as the precision matrix. The prior pdf of $\mathbf{u}$ is:

$$p(\mathbf{u}) = \mathcal{N}(\mathbf{u}; \mathbf{0}, (\alpha \mathbf{Q}^\mathbf{T} \mathbf{Q})^{-\mathbf{1}}) \quad (12)$$

where $\alpha = (\alpha_x \alpha_y)^T$, whereas the conditional pdf:

$$p(\mathbf{d}|\mathbf{u}) = \mathcal{N}(\mathbf{d}; -\mathbf{G}\mathbf{u}, \gamma^{-\mathbf{1}} \mathbf{I}). \quad (13)$$

Parameters α and γ, which control the precision and, consequently, the distribution of model parameters, are called *hyperparameters*. From this point we can proceed in two ways.

The simplest is to assume that these hyperparameters are *spatially constant*. This in effect implies that the statistics of both the residual $\varepsilon(\mathbf{s})$ in (2) and $\mathbf{Q}\mathbf{u}$ are Gaussian independent identically distributed. This is clearly an oversimplification of reality. The residuals at areas of large deformations will be larger since the linearization used in (2) would be less accurate than in areas of small deformations. Furthermore, in

areas where we have abrupt changes of $\mathbf{u}$ the values of $\mathbf{Qu}$ will be larger than in areas of smooth changes of $\mathbf{u}$.

However, in this case it is very simple to obtain the MAP estimates. Indeed by minimizing the negative log-posterior distribution:

$$-\ln p(\mathbf{u}|\mathbf{d}) \tag{14}$$

with respect to u, we obtain the solution

$$(\gamma \mathbf{G}\mathbf{G}^{\mathbf{T}} + \alpha \mathbf{Q}^{\mathbf{T}}\mathbf{Q})\mathbf{u} = -\gamma \mathbf{G}\mathbf{d} \tag{15}$$

The above linear system is approximately solved iteratively using the CGS method. This time though, apart from the source image, we also update the values for the parameters γ, α, through the following equations, obtained by minimizing again (14) with respect to γ , α_x and α_y respectively:

$$\gamma = \frac{N}{\| \mathbf{d} + \mathbf{G}\mathbf{u} \|^2}, \tag{16}$$

$$\alpha_x = \frac{N-1}{\| \mathbf{Q}\mathbf{u}_\mathbf{x} \|^2}, \tag{17}$$

and

$$\alpha_y = \frac{N-1}{\| \mathbf{Q}\mathbf{u}_\mathbf{y} \|^2} \ . \tag{18}$$

In order to overcome the above mentioned difficulties of the spatially invariant model we impose spatial adaptivity. In other words, the parameters of our model are spatially varying taking different values for each pixel location and it is possible to express them by the following vectors: $\alpha_\mathbf{x} = (\alpha_{\mathbf{x1}}\alpha_{\mathbf{x2}}...\alpha_{\mathbf{xn}})^{\mathbf{T}}$, $\alpha_\mathbf{y} = (\alpha_{\mathbf{y1}}\alpha_{\mathbf{y2}}...\alpha_{\mathbf{yn}})^{\mathbf{T}}$ and $\gamma = (\gamma_\mathbf{1}\gamma_\mathbf{2}...\gamma_\mathbf{n})^{\mathbf{T}}$. Equations (12), (13) then become:

$$p(\mathbf{u}) = \mathcal{N}(\mathbf{u}; \mathbf{0}, (\mathbf{Q}^{\mathbf{T}}\mathbf{A}\mathbf{Q})^{-\mathbf{1}}) \tag{19}$$

and

$$p(\mathbf{d}|\mathbf{u}) = \mathcal{N}(\mathbf{d}; -\mathbf{G}\mathbf{u}, \mathbf{\Gamma}^{-\mathbf{1}}) \tag{20}$$

where

$$\mathbf{A} = diag\{\alpha_{x1}, \alpha_{x2}, ..., \alpha_{xN}, \alpha_{y1}, \alpha_{y2}, ..., \alpha_{yN}\} \tag{21}$$

and

$$\mathbf{\Gamma} = diag\{\gamma_1, \gamma_2, ..., \gamma_N, \gamma_1, \gamma_2, ..., \gamma_N\} \ . \tag{22}$$

In such case, the proposed model will have $3N$ parameters to be estimated from N observations. Clearly such model although it has many advantages and capture the spatially varying nature of the residual and $\mathbf{Qu}$ also overfits the data and can not generalize [4]. For this purpose, we follow the Bayesian paradigm and add one more layer to our model. In other words, we assume $(\gamma_i, \alpha_{xi}, \alpha_{yi})_{i=1,...N}$ to be random variables and to follow a Gamma pdf parameterized by l, m, p, q_x, q_y:

$$p(\gamma_i) \propto \gamma_i^{\frac{l-2}{2}} exp^{-m(l-2)\gamma_i} \tag{23}$$

$$p(\alpha_{xi}) \propto \alpha_{xi}^{\frac{p-2}{2}} exp^{-q_x(p-2)\alpha_{xi}} \tag{24}$$

and

$$p(\alpha_{yi}) \propto \alpha_{yi}^{\frac{p-2}{2}} exp^{-q_y(p-2)\alpha_{yi}} \ . \tag{25}$$

We choose the Gamma distribution for the hyperparameters because it is the conjugate prior for the precision of a univariate Gaussian [4]. Furthermore, we chose this parametrization for the Gamma pdf because of its intuitive interpretation [6]. Minimizing (14) this time leads to the following linear system of equations:

$$(\mathbf{G}\mathbf{\Gamma}\mathbf{G}^{\mathbf{T}} + \mathbf{Q}^{\mathbf{T}}\mathbf{A}\mathbf{Q})\mathbf{u} = -\mathbf{G}\mathbf{\Gamma}\mathbf{d}, \tag{26}$$

with the following update scheme for the *spatially variant hyperparameters*:

$$\gamma_i = \frac{l-1}{(\mathbf{d} + \mathbf{G}\mathbf{u})_i^2 + 2m(l-2)} \tag{27}$$

$$\alpha_{xi} = \frac{p-1}{(\mathbf{Q}\mathbf{u}_\mathbf{x})_i^2 + 2q_x(p-2)} \tag{28}$$

and

$$\alpha_{yi} = \frac{p-1}{(\mathbf{Q}\mathbf{u}_\mathbf{y})_i^2 + 2q_y(p-2)} \ . \tag{29}$$

The role of the Gamma pdf becomes apparent by observing the above equations. For example when the deformation field becomes smooth the first term of the denominator of (28) and (29) becomes zero. Thus, without the Gamma pdf ($q_x, q_y = 0$ and $p = 2$) the estimates for α_{xi} and α_{yi} become unstable.

Parameters l and p may take values within the interval $(2, +\infty)$. Their choice affects our model in the following way. Consider for example equation (28): when p takes very close to 2, the second term in the denominator ensures that α_{xi} depends on only on $(\mathbf{Q}\mathbf{u}_\mathbf{x})_i^2$ and thus the Gamma hyperprior is non-informative since the estimates of α_{xi} and α_{yi} depend only on the data. On the other hand, if we assign a large values to p, the second term in the denominator of (28) and (29) dominates. Then, the estimates of α_{xi} and α_{yi} do not depend on the data and have the same value for all spatial locations. As a result our model degenerates to a spatially invariant model. Parameters m, q_x, q_y are extracted from the data, since it turns out that they are proportional to the variances of $(\mathbf{d} + \mathbf{G}\mathbf{u})$, $(\mathbf{Q}\mathbf{u}_\mathbf{x})$ and $(\mathbf{Q}\mathbf{u}_\mathbf{y})$ respectively.

3. EXPERIMENTAL RESULTS

Intensity similarity measures between the deformed source image and the target image are widely used criteria while evaluating a deformable registration algorithm. The main disadvantage of these criteria is that they do not provide any information about the topology preservation during the transformation. In this study, we used an alternative evaluation scheme, which combines the quantitative measurement of the intensity differences, with the qualitative estimation of the topological characteristics of the transformation.

A deformation field $\mathbf{u}$ is topologically coherent when it is "smooth". In that case the deformation vector for neighboring pixels must be similar. As a result, the spatial gradient of the field should not take large values. Based on the above, we define the *smoothness* of the deformation field as:

$$S = \frac{1}{\| \nabla \mathbf{u} \|} \tag{30}$$

We also define an *error* in the intensity matching between the deformed source image and the target image as:

$$E = \frac{1}{N} \sum_{i=1}^{N} | \ b_i^* - a_i \ | \tag{31}$$

where we remind that $\mathbf{b}^*$ is the deformed source image. Given (30) and (31) the fraction $\frac{E}{S}$ will clearly take smaller values, as the deformation either introduces smaller error or becomes smoother.

In this experiment, we use a 2D image, which is a brain MRI slice as the target image. The target image is deformed using a known non-linear formula. We produced two source images, one with relatively small deformation and one with a relatively large deformation. We registered the source images to the target image using the stationary and the non stationary algorithms described in section 2.

At first, we perform one iteration of the constrained optical flow equation (9), selecting one value for the constant weight α. The resulting deformation field is then used to initialize the hyperparameters (27)-(29) for the non-stationary equation (26), which we let it iterate until convergence. The results of this scheme are shown in figures 1 and 2, for the small and the large deformation respectively. We observe that there is a significant improvement in the intensity differences for both deformations. For the large deformation, we notice that the algorithm fails to fully align the two images in regions where the initial error is too large. This is caused by the regularization term, which does not allow non-continuous mapping between neighboring pixels. A reduction in the constraint weight would produce a result with less error, but not topologically coherent. For the small deformation, it is hard to obtain a good visualization of the differences between the images. Nevertheless, there are many non-zero values and a deformation does indeed take place, as it is confirmed by the differences in the final result when we additionally let the constrained optical flow algorithm converge.

We also calculate the values of the fraction $\frac{E}{S}$ for both methods. The results, for various initial values of α, are illustrated in figure 3, for the small (a) and the large (b) deformation. It becomes clear from the above figure that applying the non-stationary method to the problem provides better results, as far as our evaluation criterion is concerned. It is notable that independently from the initial, arbitrary, choice of α, spatial variance seems to either reduce the error of the registration or increase the smoothness of the deformation field, or both. In that way, the bias introduced by the non-automatic initialization of the constraint weight factor (9) may be reduced. Moreover, we observed that the execution time is shorter for the non-stationary method, up to a percentage of 70%. This can prove very crucial during the registration of high-dimensional images, especially in the 3D case.

4. CONCLUSION

In this paper, we presented a method for non rigid image registration based on a spatially variant model. The model imposes smoothness on the deformation field which is assumed to be a random variable conditioned on the observations (inter-image differences). The obtained registration errors are inferior to the errors provided by the simple stationary model. Future directions of this study are the extension of the method to 3D MRI registration where the model non stationarity will provide a more clear advantage. Also, comparison with other state of the art methods [3, 5], though difficult due to absence of golden standards and ground truth, is a key element and an issue of ongoing research.

REFERENCES

[1] S. Allassonniere, Y. Amit, and A. Trouvé. Towards a coherent statistical framework for dense deformable template estimation. *Journal of the Royal Statistical Society (B)*, 69(1):3–29, 2007.

[2] Y. Amit. A nonlinear variational problem for image matching. *SIAM Journal of Scientific Computing*, 15:207–224, 1994.

[3] M. F. Beg, M. I. Miller, L. Younes, and A. Trouvé. Computing metrics via geodesics on flows of diffeomorphisms. *International Journal of Computer Vision*, 61(2):139–157, 2005.

[4] C. M. Bishop. *Pattern Recognition and Machine Learning*. Springer Science and Business Media, LLC, New York, USA, 2006.

[5] Y. Cao, M. I. Miller, R. L. Winslow, and L. Younes. Large deformation diffeomorphic metric mapping of vector fields. *IEEE Transactions on Medical Imaging*, 24(9):1216–1230, 2005.

[6] J. Chandas, N. P. Galatsanos, and A. Likas. Bayesian restoration using a new hierarchical directional continuous edge image prior. *IEEE Transactions on Image Processing*, 15(10):2987–2997, 2006.

[7] G. E. Christensen, M. I. Miller, M. W. Vannier, and U. Grenander. Individualizing neuro-anatomical atlases using a massively parallel computer. *IEEE Computer*, pages 32–38, January 1996.

[8] W. Crum, T. Hartkens, and D. Hill. Non-rigid image registration: theory and practice. *British Journal of Radiology*, 77:S140–S153, 2004.

[9] C. Davatzikos and R. N. Bryan. Using a deformable surface model to obtain a shape representation of the cortex. *IEEE Transactions on Medical Imaging*, 15:785–795, 1996.

[10] G. Demoment. Image reconstruction and restoration: overview of common estimation structures and problems. *IEEE Transactions on Signal Processing*, 37:2024 – 2036, 1989.

[11] M. Fornefett, K. Rohr, and H. S. Steihl. Radial basis functions with compact support for elastic registration of medical images. *Image and Vision Computing*, 19:87–96, 2001.

[12] C.A. Glasbey and K.V. Mardia. A penalized likelihood approach to image warping. *Journal of the Royal Statistical Society (B)*, 63(3):465–514, 2001.

[13] W. Lu, M. L. Chen, G. H. Olivera, K. J. Ruchala, and T. R. Mackie. Fast free-form deformable registration via calculus of variations. *Physics in Medicine and Biology*, 49:3067–3087, 2004.

[14] S. Marsland and C. J. Twining. Constructing diffeomorphic representations for the groupwise analysis of nonrigid registrations of medical images. *IEEE Transactions on Medical Imaging*, 8:1006–1020, 2004.

[15] J. Modersitzki. *Numerical methods for image registration*. Oxford University Press, 2003.

[16] O. Musse, F. Heitz, and J. P. Armspach. Topology preserving deformable image matching using constrained hierarchical parametric models. *IEEE Transactions on*

(a) (b) (c) (d) (e)

Figure 1: Registration example with relatively small image deformations. (a) Reference image, (b) image to be registered to the reference image, (c) difference between the unregistered images, (d) registered image, (e) difference between the registered image and the reference image.

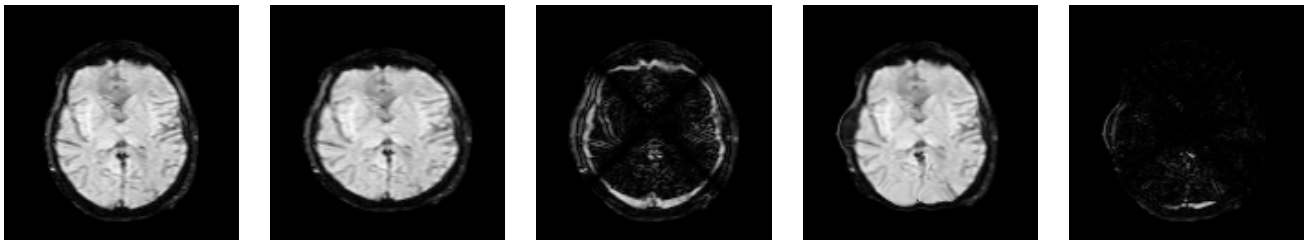

(a) (b) (c) (d) (e)

Figure 2: Registration example with relatively large image deformations. (a) Reference image, (b) image to be registered to the reference image, (c) difference between the unregistered images, (d) registered image, (e) difference between the registered image and the reference image.

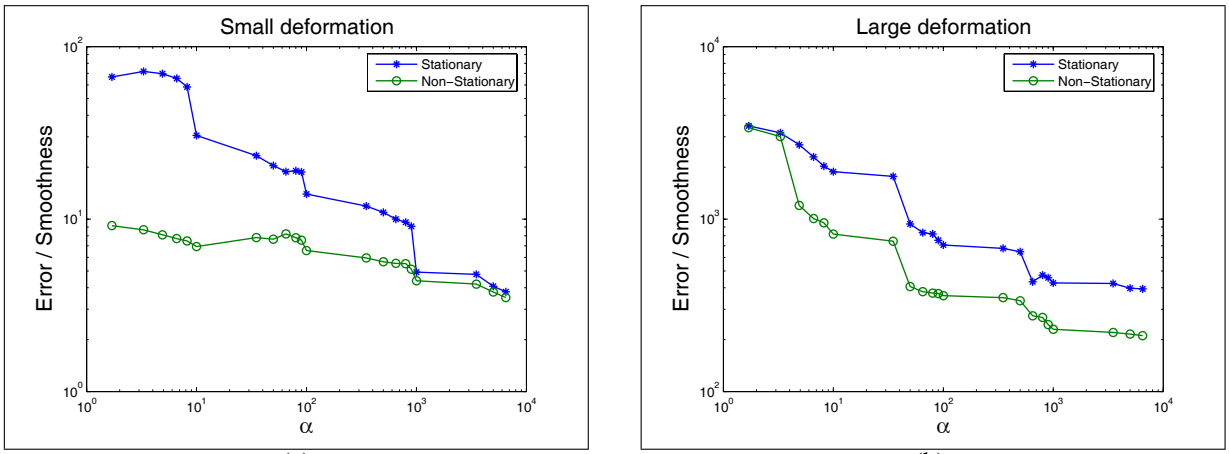

(a) (b)

Figure 3: Registration error over smoothness curves for various values of the parameter α for the stationary and the non stationary registration models. (a) Small deformation (fig. 1), (b) large deformation (fig. 2).

Image Processing, 10:1081–1093, 2001.

[17] F. Richard, A. Samson, and C. Cuénod. A SAEM algorithm for the estimation of template and deformation parameters in medical image sequences. Technical report, Université Paris Descartes, MAP-5, 2007.

[18] D. Rueckert, L. I. Sonoda, C. Hayes, D. L. G. Hill, M. O. Leach, and D. J. Hawkes. Nonrigid registration using free-form deformations: Application to breast MR images. *IEEE Transactions on Medical Imaging*, 18:712–721, 1999.

[19] J. P. Thirion. Image matching as a diffusion process: An analogy with Maxwells demons. *Medical Image Analysis*, 2:243–260, 1998.

[20] A. Tikhonov and V. Arsenin. *Solution of Ill-posed Problems*. Winston & Sons, Washington, USA, 1977.

[21] Y. T. Wu, T. Kanade, C. C. Li, and J. Cohn. Image registration using wavelet-based motion model. *International Journal of Computer Vision*, 38:129–152, 2000.